Electric Power Systems Research 206 (2022) 107833

Contents lists available at ScienceDirect

Electric Power Systems Research

journal homepage: www.elsevier.com/locate/epsr

Analysis of the use of the Hanning Window for the measurement of interharmonic distortion caused by close tones in IEC standard framework.

Angel Arranz-Gimon [a], Angel Zorita-Lamadrid [b], Daniel Morinigo-Sotelo [b], Oscar Duque-Perez [b,*]

[a] Department of Electronic Technology, Universidad de Valladolid, Valladolid 47011, Spain
[b] ADIRE, ITAP, Department of Electrical Engineering, Universidad de Valladolid, Valladolid 47011, Spain

ARTICLE INFO

Keywords:
Electric power quality
Harmonic distortion
Standard IEC61000–4–7
Hanning window
Time aggregation
Adjustable speed drive (ASD)
Induction motor

ABSTRACT

The widespread use of devices based on power electronics and other nonlinear loads has led to an increase in harmonic distortion that affects the quality of power systems. Therefore, the correct measurement of harmonic and interharmonic content is necessary. The International Electrotechnical Commission (IEC) standards define the concepts of spectral and time grouping required for such measurements. This paper demonstrates that the procedures defined in the IEC standards are not sufficiently accurate when several close interharmonic tones interact due to the lack of stability of the values that the Discrete Fourier Transform obtains in each sampling window, and to the inaccuracy in the measurement of interharmonic groups and rates when using the Hanning window. This paper proposes novel solutions based on time aggregation and the use of other groupings and alternative windows. The results obtained are compared with the results produced by applying the rectangular window indicated in the standards, using sensitivity analysis varying one of the tones and using experimental results measuring the output signals of frequency inverters driving induction motors. The proposed method achieves greater accuracy and stability in the measurement of spectral groupings and their related distortion rates in signals with abundant and dispersed interharmonic content.

1. Introduction

The increased use of non-linear loads has led to a growth in harmonic distortion that affects the quality of power systems [1, 2]. Harmonics and interharmonics are generated by non-linear loads, such as power electronic converters, switching power supplies, or variable frequency drives.

In addition, the need to achieve greater energy efficiency and environmental concerns have led to an increase in the use of renewable energy equipment, such as photovoltaic [3, 4] and wind [5] installations, as well as low consumption lighting sources [6, 7], electric vehicle chargers [8, 9], and other modern household appliances. All these equipment are based on power electronic devices that cause high harmonic pollution since their high-frequency switching circuits emit distortion in the harmonic (< 2 kHz) and in the supra-harmonic frequency range (2–150 kHz) [10–12].

Harmonics and interharmonics cause unwanted effects such as overheating of equipment, network losses, flicker, interference in communications systems and misfiring of semiconductor switches. Supra-harmonic emissions also cause malfunction of control systems and digital meters and can shorten the lifetime of network components and household equipment [13–15].

Therefore, in order to avoid these problems, the correct measurement of harmonic and interharmonic content is necessary. The IEC power quality measurement standards 61000–4–7 [16] and 61000–4–30 [17] define methods for measuring and interpreting results of harmonic and interharmonic distortion in the power grid and describe the spectral groupings and the time aggregation necessary to perform such measurements.

These IEC standards indicate the use of the discrete Fourier transform (DFT) as the basic tool for harmonic analysis and requires the use of rectangular time windows (RW) of a fixed length of ten cycles for 50 Hz systems (or 12 cycles for 60 Hz networks) corresponding to approximately 200 ms and a resolution of 5 Hz. Note that DFT produces a more accurate spectral estimate when the analysed signal is stationary and the sampled window is time-synchronised to the fundamental period. However, the accuracy of DFT worsens when the length of the chosen time window is not an integer multiple of the periods of all the components contained in the signal. This is especially true in the presence of interharmonics, which are common in power electronic converter signals, producing changes in the periodicity of the waveform and greater

* Corresponding author.
E-mail address: oscar.duque@eii.uva.es (O. Duque-Perez).

https://doi.org/10.1016/j.epsr.2022.107833
Received 23 September 2021; Received in revised form 20 December 2021; Accepted 26 January 2022
Available online 2 February 2022

Nomenclature

ASD	Adjustable Speed Drive
DFT	Discrete Fourier Transform
f_1	Fundamental frequency at inverter output
gH	Harmonic Group
gIH	Interharmonic Group
H	Harmonic spectral bar
HW	Hanning Window
IEC	International Electrotechnical Commission
PWM	Pulse Width Modulation
RW	Rectangular Window
s	Slip of a motor
SgH	Harmonic Subgroup
SgIH	Interharmonic Subgroup
THD	Total Harmonic Distortion
TIHD	Total Interharmonic Distortion Group
TIHDS	Total Interharmonic Distortion Subgroup
tw	Analysis or sampling window

sensitivity to desynchronization problems [18]. In these cases, spectral leakage is generated, which leads to misleading measurements of the harmonic content of the analysed signal.

To reduce such spectral leakage and its effects, IEC 61000–4–7 [16] points out several procedures:

- The correct synchronisation of the acquisition windows to the fundamental.
- The use of Hanning windows (HW) instead of rectangular ones in case of loss of synchronism.
- The use of frequency and time groupings.

However, the use of HW leads to a worsening of the resolution when measuring close tones, despite its better performance in reducing the effects of the leakage between distant tones. This is due to the large width of the main lobe of this window, which causes an appreciable gain in the spectral sidebands at the frequency of the considered tone (at ±5 Hz for 200 ms windows) [19].

In terms of groupings, time grouping solves part of the loss of information that the spectral leakage produces [20]. However, these time groupings (as well as the duration of the sampling windows) are specified in the IEC standards for the analysis of network signals in general, but these standards do not address the selection of a suitable aggregation time for harmonic analysis adapted to each type of signal [21–26].

These topics have been addressed in the literature. Several measurement methods based on DFT in the IEC standard framework have been described [21, 27–29], and also more recently for the supra-harmonic frequency range [30–32]. Other non-DFT methods have been proposed for the estimation of harmonics and interharmonics [33, 34], such as parametric, non-parametric and hybrid approaches. Nonetheless, DFT remains the simplest, fastest and most robust technique for this purpose [35].

Methods to reduce spectral leakage have been also proposed in the literature such as:

- The use of interpolation algorithms.
- The adjustment of the sampling window size to achieve synchronisation with the fundamental frequency of the signal.

However, interpolation algorithms are not accurate when there are interharmonic components in the signal [36]. Besides, the time resolution should be adapted to the characteristics of the analysed signal [36, 37]. For example, when measuring the output of an inverter, the size of 200 ms (suitable for network signals) is no longer adequate.

In [18–20, 38–40], it is compared how RW and HW minimize the influence of leakage, comparing the results for the 61000–4–7 frequency groupings, but they do not consider the 61000–4–30 time groupings, nor both spectral and time groupings simultaneously.

The purpose of this article, therefore, is to demonstrate the existence of this problem of spectral leakage and to propose a solution. Thus, first of all, it will be shown that there is a problem, due to spectral leakage, in obtaining IEC-based frequency groupings and distortion rates in the variability (and unreliability) of the values found in successive sampling windows after applying DFT, when close tones interact with at least one interharmonic tone of a relatively large magnitude. This problem causes the RMS values obtained to depend excessively on the specific sampling window chosen, and on the relative position between the interharmonic tones, leading to unreliable results.

And secondly, it will be shown how, when using HW, a second problem appears: the interharmonic groups (and related distortion rates) can absorb part of the energy of their adjacent harmonics, due to the sidebands of the HW, producing a new error to be added to the aforementioned error due to spectral leakage.

Solutions to both problems are presented in this paper. Thus, as a solution to the first problem, it will be shown how aggregation over time can reduce the influence of the leakage and bring the results closer to the ideal ones. It is also shown that the aggregation time required is greater for signals containing close interharmonics, such as signals from frequency variators [41], especially the ones that use modulations such as random carrier [42, 43] or closed-loop controls [44], and even more if they feed faulty motors (resulting in greater interharmonic content [45, 46]). And as a solution to the second problem, techniques based on using another type of window or frequency grouping are proposed, including in the latter case an improvement in the frequency resolution to compensate for the error committed when changing the grouping.

Accordingly, the main contribution of the proposed methodology consists in increasing the accuracy of the interharmonic grouping quantification process using DFT by selecting the most appropriate aggregation times, window types, resolutions and grouping sizes, and also extends its use to obtaining rates that correctly assess interharmonic distortion at the output of equipment with a strong interharmonic content, such as variable frequency drives that feed induction motors.

The rest of the paper is organised as follows. In Section 2, the amplitudes of the different harmonic groupings defined in the standard are studied when the position of a tone is varied and when two tones interact, as well as the problem of imprecision in the measurement of interharmonic groups when using HW. Section 3 verifies that, when close tones interact, the aggregation over time increases the reliability of the measurement and, in the case of interharmonic group measurement using HW, other proposed techniques are also necessary. Section 4 describes the case study, showing that the measurement problems described in previous sections appear. Section 5 presents the discussion of the results of the previous section, showing that the proposed methodology satisfactorily solve the measurement problems. Finally, Section 6 shows the main conclusions of this work.

2. Frequency response of IEC harmonic groupings using RW and HW windows

This section studies the inaccuracy in the measurement of the harmonic groupings defined in the IEC standard due to amplitude variations over successive sampling windows. First, the influence of the position of the analysed tone is considered, and then, the interaction of two tones is explored, both with harmonic groupings and in the special case of interharmonic groups with adjacent harmonics.

2.1. Analysis for a single tone

In this subsection, a single sweep tone of amplitude one is

considered. Fig. 1 is obtained applying DFT on each sampling window, using RW and HW with a window length of 200 ms (5 Hz separation between spectral bars). Fig. 1 shows the amplitudes of the harmonic groupings defined in the IEC standard: individual spectral bar (H_1), harmonic subgroup (SgH_1) and harmonic group (gH_1).

For frequencies multiples of 5 Hz, the correct value is measured (1 Vrms inside the groupings and 0 outside), since there is no leakage, as the periods fit an integer number of times in the 0.2 s window used. For interharmonic frequencies, there is leakage and part of the energy is released towards frequencies outside the grouping when the tone is inside, or into the grouping when it is outside.

The values obtained are further away from the ideal, the larger the spectral leakage generated by the tone, increasing the error as the tone approaches the central positions between spectral bars, and decreasing as it approaches the positions of the spectral bars.

Spectral leakage produces more pronounced effects with RW, while with HW the response is much flatter and closer to the ideal in the inner zones and in the zones furthest away from the harmonic groupings considered (see Fig. 1), due to HW being less affected by remote leakage. On the other hand, the response with RW is better in the transition zones between groupings (for example, in Fig. 1, zones 40–45 Hz and 55–60 Hz, for harmonic subgroup SgH).

To understand the difference between the results obtained with RW and HW, it should be remembered that RW presents a narrower main lobe (with better resolution between close tones in frequency), but its side lobes are the largest and with the slowest attenuation (with the worst interference due to spectral leakage between non-close tones). On the other hand, HW is characterised by a worse frequency resolution than RW, with a main lobe width twice that of RW, but with a better behaviour of its side lobes, of small value and fast attenuation, thus reducing the effect of interference due to spectral leakage. In addition, due to the width of its main lobe, HW has a gain "−0.5″ in the spectral sidebands distanced ±5 Hz of the tone frequency. Therefore, with HW and for groupings adding up to several consecutive spectral bars, a "group gain" [19] value of $\sqrt{1.5}$ must be considered.

2.2. Analysis of the interaction between a fixed harmonic and a tone with variable position

For the case of a single tone, the amplitudes obtained by applying the DFT remain constant throughout the successive windows analysed. However, when several nearby tones interact and at least one of them is interharmonic, there is a significant variation in the amplitudes obtained over the consecutive windows analysed. This amplitude variation is greater the smaller the distance between the interacting tones.

That is the case for a signal composed of harmonic and interharmonic tones generating spectral leakage, as shown in Fig. 2. When the vector representing the leakage is added to the harmonic vector, the total vector absolute value is different for successive sampling windows. This is because the leakage vector is rotating, as it changes its phase shift with respect to the beginning of each analysis window, and the harmonic vector is fixed, as the harmonic period is a multiple of the analysis window and therefore does not change its phase at the beginning of the window [21]. This means that the amplitude of the total vector at the harmonic spectral position can vary substantially between acquisition windows.

Fig. 3 shows the case of a harmonic tone of unit amplitude, fixed at 50 Hz, interacting with another tone of variable sweep or frequency between 0 and 100 Hz and of the same amplitude. The amplitudes obtained by applying DFT, over three successive analysis windows (tw1–tw3), are plotted for the harmonic subgroups obtained using both RW and HW. It can be seen that the greatest variations, depending on the variable frequency tone position and the specific time window, occur at the positions where the interacting tones are closest to each other (≈ 50 Hz). And these variations are more extended for RW, due to its lower attenuation which causes a greater influence of the distant leakage.

The simulations of Fig. 4 have been obtained applying a 0.2 s sampling window (5 Hz) without aggregation, and with an offset of 90° between tones. The zone of greatest interaction between tones is around 50 Hz (when sweep and harmonic tones are closer). The oscillation in that zone is more extended for HW (to the spectral sidebar zones, 40–60 Hz), no doubt due to the greater interaction of the HW's own sidebands, both those of the spectral sidebar of the harmonic position (45 and 55 Hz) and of the sweep tone (the upper sideband of a 40 Hz sweep tone would be at 45 Hz and would be added to the lower sideband of the 50 Hz harmonic bar, also located at 45 Hz; analogously for the lower sideband of a 60 Hz sweep tone). For frequencies below 40 or above 60 Hz, the values are more stable, although the oscillations are larger for RW.

Thus, if a single window is analysed: the results depend on the tone

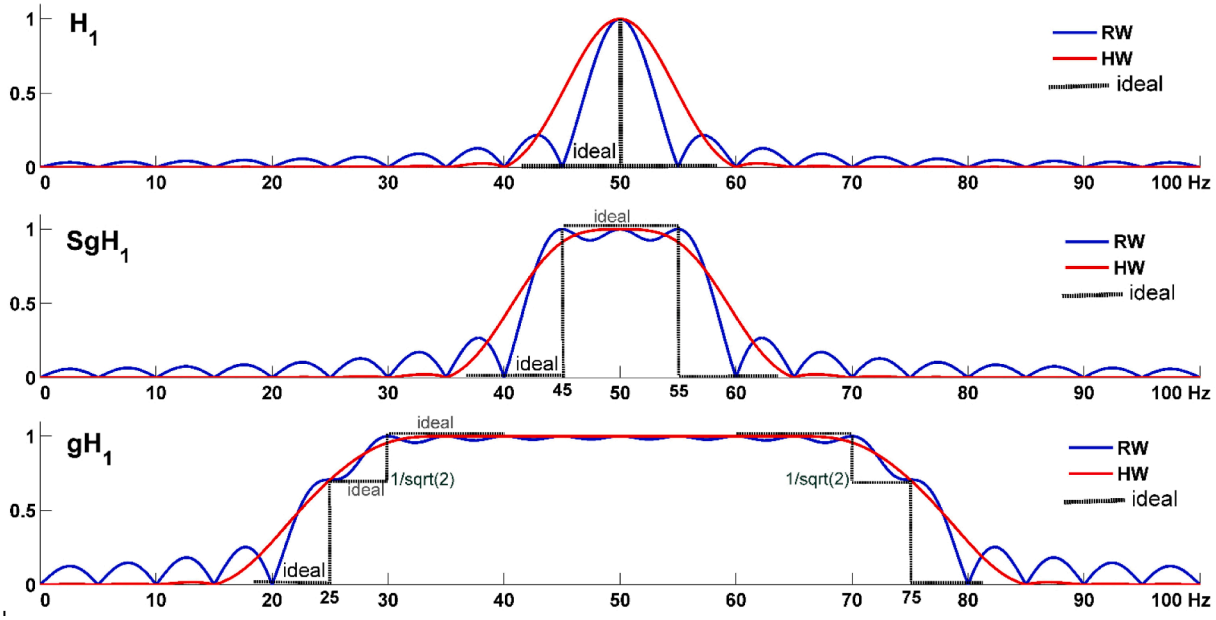

Fig. 1. Individual spectral bar (H1), harmonic subgroup (SgH1) and harmonic group (gH1) for a single sweep tone (blue RW, red HW, black ideal). A window length of 200 ms is considered.

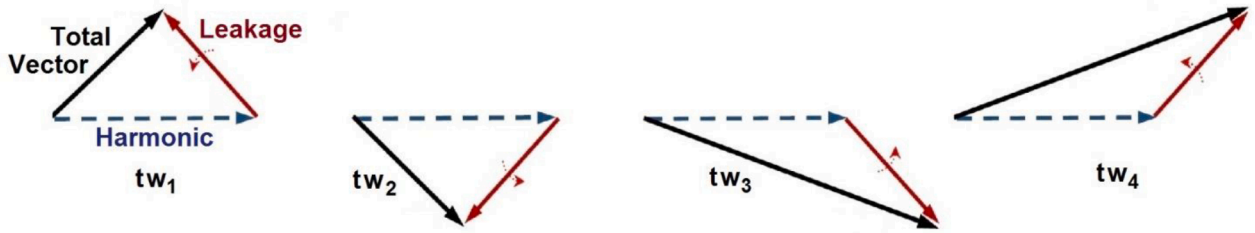

Fig. 2. Vector evolution over successive 0.2 s sampling windows of the total RMS vector measured at 50 Hz resulting from the sum of a harmonic at the same position and the leakage generated from a nearby interharmonic at 51.25 Hz (total vector in black, harmonic in dashed blue, spectral leakage in red).

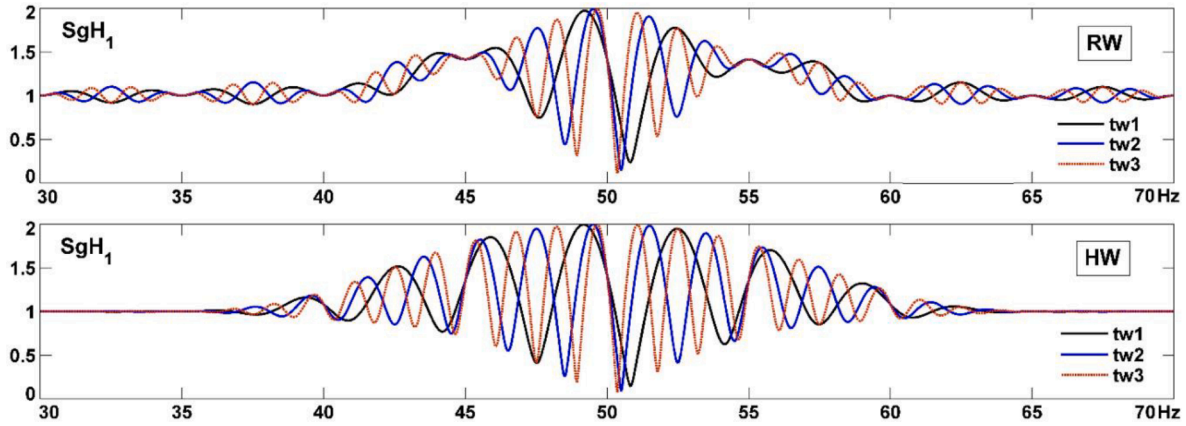

Fig. 3. RMS values of harmonic subgroups for a sweep unit tone and a fixed harmonic at 50 Hz, for 3 successive tw1-tw3 windows without aggregation using RW and HW.

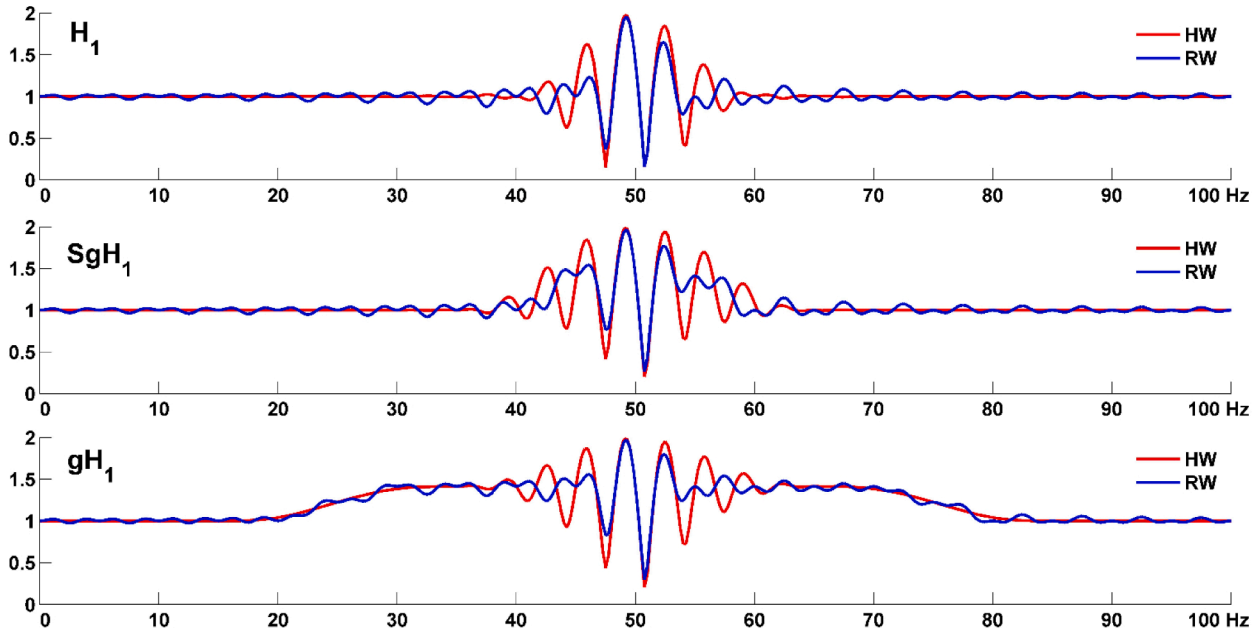

Fig. 4. RMS values of harmonic groupings (individual spectral bar (H1), harmonic subgroup (SgH1) and harmonic group (gH1)) for a sweep unit tone and a fixed harmonic at 50 Hz, with a 0.2 s window without aggregation, using RW (blue) and HW (red).

considered, with greater interaction and amplitude variations when both tones are close together, as shown in Fig. 4. And, for a specific tone, the results also change between successive windows, as shown in Fig. 3.

This can be generalised for any number of interharmonic tones, with maximum amplitude variations, when applying the DFT in successive windows, in the spectral bars close to the interacting and leakage generating tones, versus smaller changes in the more distant ones. Moreover, the resulting total vector can generally range between the sum of the moduli or their difference, as a function of the leakage vector phase angle.

2.3. Problems in the particular case of the measurement of interharmonic groups with HW

This section presents an additional problem, which may arise when using HW, due to the inaccuracy in the measurement of interharmonic groups and their related rates. This problem is due to the fact that the interharmonic groups, and the distortion rates that contain these groups, can absorb part of the energy of their adjacent harmonics, due to the sidebands of HW. This gives rise to a new error, to be added to the aforementioned error due to spectral leakage.

Fig. 5(a) shows the interharmonic group gIH1 (including the spectral bars between 55 and 95 Hz), obtained with both RW and HW, as a function of a single unit tone of varying frequency. The behaviour is similar to that obtained with the harmonic groupings in Section 2.1, and therefore the same observations can be made regarding the influence of spectral leakage for both RW and HW. As this is a single tone, no amplitude variations are present over successive analysis windows, and the values obtained depend on the position or frequency of the tone, but not on the time window chosen for its analysis.

In Fig. 5(b), a second harmonic tone is added at the 50 Hz position. Thus, the interharmonic group gIH_1 is plotted again against the same variable and fixed harmonic tones at 50 Hz as in the previous section, now 180° out of phase. This second tone should not influence the amplitudes measured with the DFT, since being harmonic, it does not emit spectral leakage and the tone itself is not contained within the spectral bars of the interharmonic group being measured.

Therefore, with RW (blue graph), the same values are obtained as in Fig. 5(a) with a single tone. Besides, in Fig. 5(b), the values remain constant window after window of analysis, because only variable frequency interharmonic tone (which produces leakage) can exist in the area of the measured interharmonic group (and the fixed harmonic, located outside that area, does not produce leakage, it can only receive it). This way, there is no interaction between components of different tones.

On the other hand, since the width of the HW's lobe is double the RW's (with a "−0.5″ gain in the spectral sidebands) there are oscillations of values along successive windows (as can be seen in the dashed plots in Fig. 5(b) for the first 3 windows analysed using HW). This is due to the interactions between one of the harmonic sidebands and the other variable tone. This is again the case of several components with different rotational speed of their leakage and therefore different amplitude values in their sum vector in each successive window of analysis.

3. Improvement of the frequency response of spectral groupings when close tones interact

This section presents the way to attenuate the effects of amplitude variations in time due to the interaction between near tones, described in the previous section, by using the aggregation in time of the RMS values found in the successive windows analysed. In this way, it is possible to stabilise and improve the reliability of the values obtained. This section also presents the solution to the additional problem observed in Section 2.3, which may arise when using HW, due to the inaccuracy in the measurement of interharmonic groups, which requires not only the use of time aggregation to solve it, but also other proposed techniques.

3.1. Improvement of the frequency response of harmonic groupings by time aggregation

In Section 2 it was shown that the interaction of spectral leakage between neighbouring tones causes amplitude changes in the RMS values found over consecutive analysis windows. To correct this problem, it is proposed to aggregate over time the RMS values found in consecutive windows. Time aggregation is performed using the square root of the arithmetic mean of the squared input values.

By means of time aggregation, the harmonic content of each spectral bar is stabilised and approximates the common RMS of all the components that are added in that bar. Fig. 6 shows a harmonic subgroup obtained with and without aggregation.

In general, values closer to the ideal common RMS value are obtained when increasing the number of aggregated windows. In areas where close tones of similar amplitudes interact, the differences between values obtained in individual windows and the aggregates are larger and, therefore, more aggregation time is needed. This can be seen in the area around 50 Hz in Fig. 6 by comparing the graphs from the lowest to the highest number of aggregated windows.

Therefore, if a proper time aggregation is chosen, results like those shown in Fig. 7 can be obtained for the harmonic groupings. It should be noted that, in general, the results obtained using time aggregation with RW are better (closer to the ideal values without spectral leakage, shown in Fig. 7 in dotted black) in the transition zones between groups. Using HW, the results are better in the inner zones and in the zones furthest away from the measured grouping (similarly to the single-tone case). Results using time aggregation are even better that the ones obtained for a single tone without aggregation, especially in the areas far from the harmonic groupings, where a smaller oscillation of values is observed (especially in the RW case).

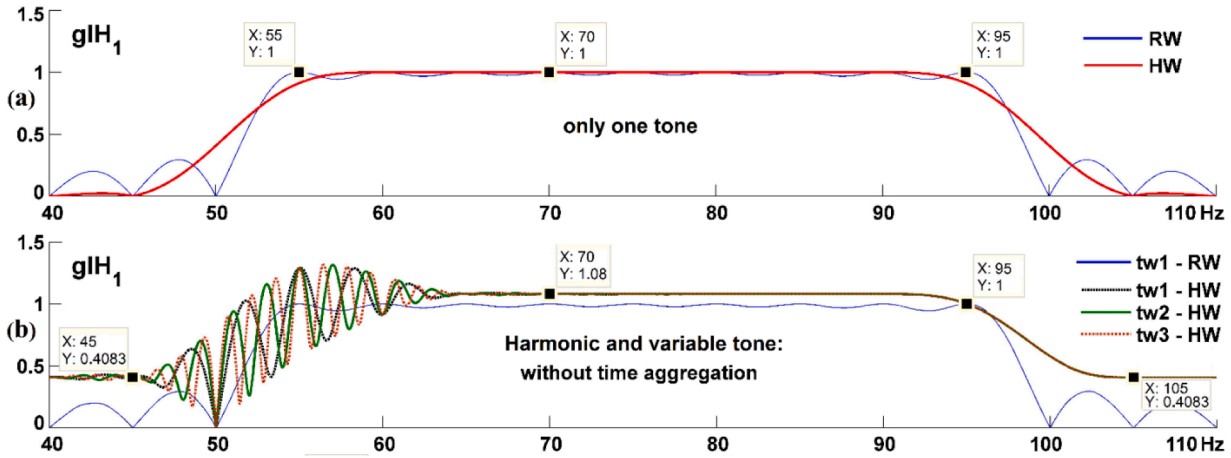

Fig. 5. Interharmonic group RMS values with HW and RW: (a) for a single sweep unit tone for one or several windows without time aggregation, and (b) with a fixed second harmonic tone at 50 Hz for the first 3 windows without time aggregation tw1-tw3.

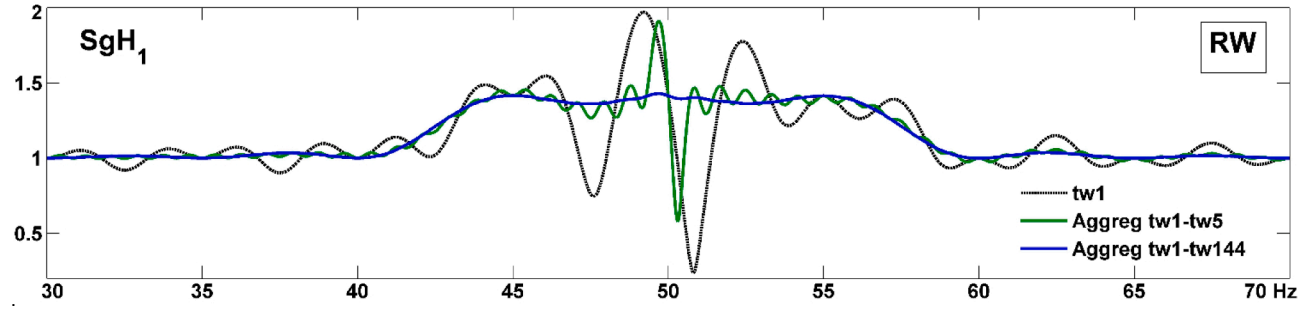

Fig. 6. RMS values of a harmonic subgroup for a sweep unit tone and a fixed harmonic at 50 Hz, for successive RW, without aggregation (black line) and with time aggregation (aggregating the first 5 windows, green line, and with a high number of windows aggregated, blue).

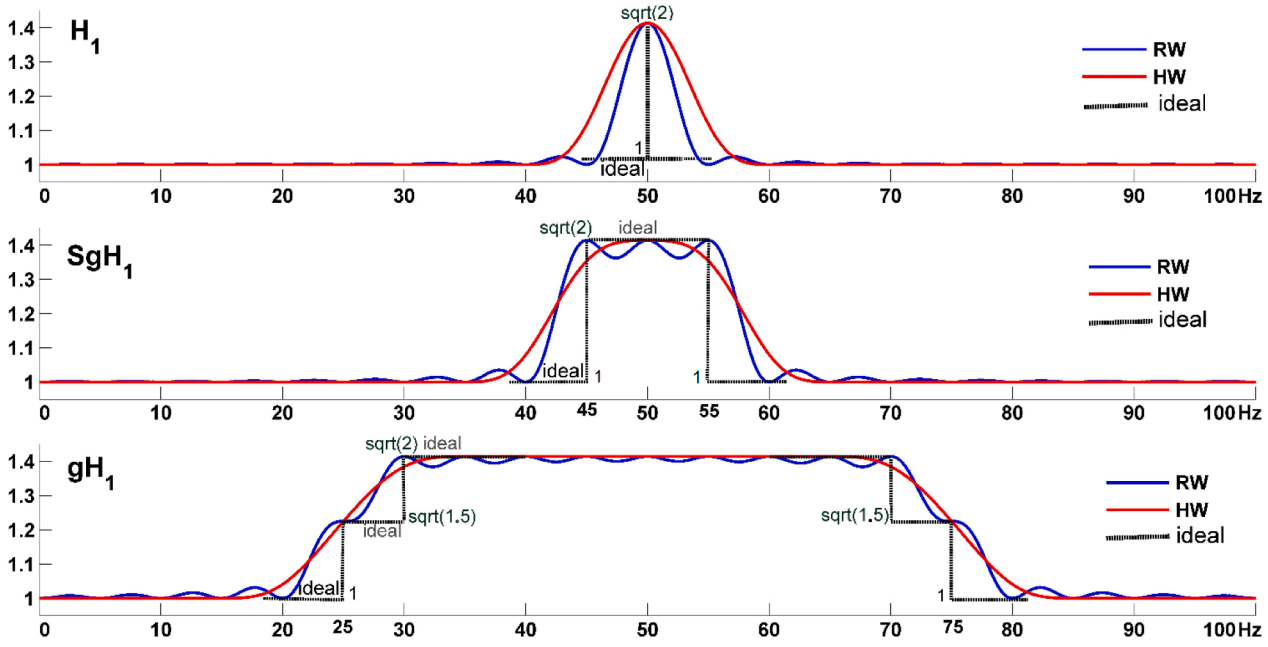

Fig. 7. RMS values of harmonic groupings (individual spectral bar (H1), harmonic subgroup (SgH1) and harmonic group (gH1)) for a sweep unit tone and a fixed harmonic, at 90°, using RW (blue) and HW (red) with time aggregation. The ideal values are shown in black.

Time aggregation is less necessary in areas where the tones are farther apart and interact less, and even unnecessary in the case of HW in these areas away from the central harmonic, as can be seen by comparing Figs. 4 and 7.

The simulated tones are vectorially summed in the positions where the spectral components due to both coincide (50 Hz in these

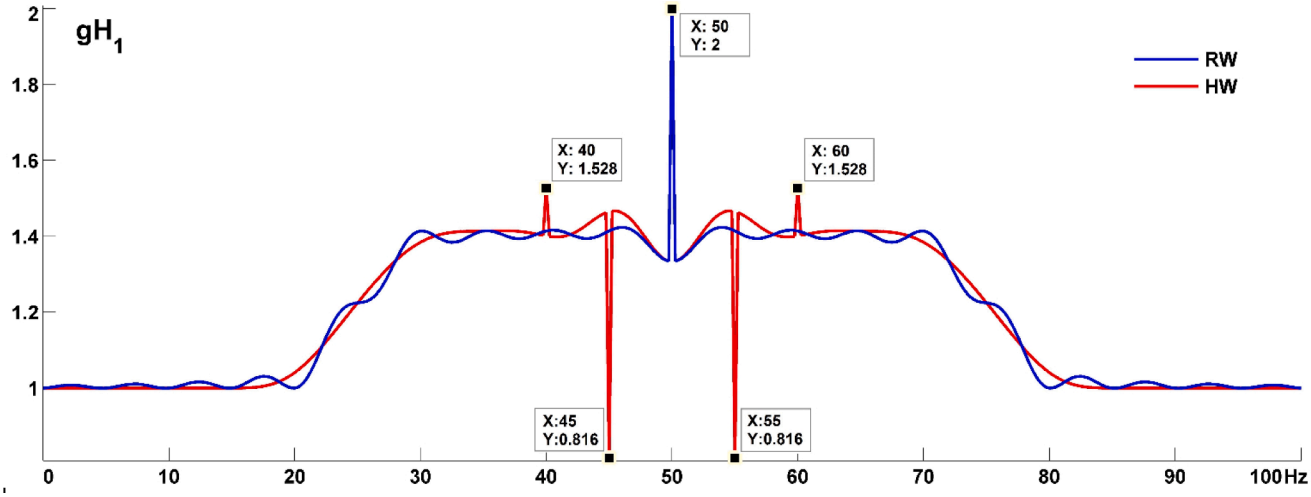

Fig. 8. RMS values of harmonic group for a sweep unit tone and a fixed harmonic, now with 0° phase shift, using RW (blue) and HW (red) with time aggregation.

simulations) and therefore the phase difference between them can give rise to a maximum (when both tones, harmonic and sweep, are at 0°, as shown in Fig. 8 for the case of a harmonic group), a minimum (when they are at 180°) or intermediate values for the rest of the phase differences. For the particular case of 90°, considered in Fig. 7, these maximums and minimums are not observed, since the total RMS value is the same, regardless of whether the tones coincide or not (the square of the vector sum and the sum of their individual squares are identical for two tones at 90°).

However, when the phase difference is not of 90°, different values appear in the position where the components of the two tones coincide than in the rest of the positions, and which depend on the specific phase difference. With HW, this occurs not only when the tone frequencies are equal (50 Hz), but also when the tones sidebands coincide, as shown in Fig. 8. Then we have singular values (or "local peaks" [19]), for the central harmonic tone (and at ±5 and ±10 Hz), due to tones main lobes interferences, being the variations maximal when the tones phase difference is 0° or 180° These local peaks can be resolved if aggregation in time is combined with the overlap between windows, as demonstrated in [21].

3.2. Improvement of the frequency response of interharmonic groupings with HW

The problem shown in Section 2.3 is again largely solved by the time aggregation of the values obtained in a suitable number of consecutive windows (red plot in Fig. 9(a)). The local peaks observed at 55 and 60 Hz are due to the interaction of the upper band of the harmonic (55 Hz) with the variable frequency tone (when it is located at 55 Hz) and with the lower band of the tone (when it is located at 60 Hz). At these frequencies, the vectors of the components that are added do not change their positions, since they differ in frequencies multiple of the resolution of 5 Hz, so their phase is always the same at the beginning of each sample window and therefore time aggregation is not sufficient to correct these values. In such cases, the use of time aggregation combined with window overlapping is required to correct these local peaks [21], as shown in Fig. 9(b).

Aggregation allows to obtain stable results, closer to the correct RMS values, but it does not avoid the displacement of values using HW (Fig. 9 (b)). In this example, the upper harmonic sideband at 55 Hz falls into the area covered by the interharmonic group and is always measured within this group, regardless of the position and offset of the other sweep tone. This is the reason why in the areas with the sweep tone outside the group (and taking into account that the other tone is always outside the group), it is obtained

$$\sqrt{(1\cdot(-0.5))^2}\Big/\sqrt{1.5} = 0.4083$$

instead of obtaining "zero", and in the flat part, inside the interharmonic group, instead of "1″, it is obtained

$$\sqrt{(1\cdot(-0.5))^2 + \left[(1\cdot(-0.5))^2 + (1\cdot 1)^2 + (1\cdot(-0.5))^2\right]}\Big/\sqrt{1.5} = 1.0801$$

The term "(1•(−0.5))" is the contribution of the sideband above the harmonic, and the remaining terms are due to the sweep tone and its two sidebands. Therefore, the shift of values using HW is due to the unwanted contribution of the upper band to the harmonic, located at 55 Hz, within the group gIH_1 (analogously for the lower band at 50 Hz, at 45 Hz, and the interharmonic group gIH_0).

This situation, in which a component outside a group is measured improperly, also occurs for interharmonics located close to the transition or boundary zone of the group under consideration.

It should be noted that, using the resolution recommended in the IEC standards, the separation between spectral bars is large and it is not uncommon that a harmonic (or other close component) may contribute with unwanted energy. Furthermore, the amplitude of the harmonics may be larger than those of the interharmonics, generating large errors when the harmonic sidebands are added to the interharmonic groups. In such cases, with harmonics close to the interharmonic groups to be measured, RW is preferable as it is closer to the desired ideal response (grey dashed plot in Fig. 9(b)).

Another possibility is to use interharmonic subgroups instead of groups (thus avoiding harmonics' sidebands). An increase of the frequency resolution (e.g. from 5 to 2.5 Hz) can compensate for the loss of accuracy using interharmonic subgroups instead of full groups. The latter is shown in Fig. 10 with the interharmonic subgroup $SgIH_1$, which aggregates the spectral bars between 60 and 90 Hz for a resolution of 5 Hz (HW in red, and RW in blue), and aggregates the bars between 57.5 and 92.5 Hz for a resolution of 2.5 Hz (HW in red, and RW in black) thus getting closer to the ideal interharmonic group.

The increase in frequency resolution also improves the measurements as can be observed in Fig. 10. Only in the areas around the spectral bars multiples of 5 Hz is the result slightly better, while the result for 2.5 Hz is much better at all other positions. The increase in frequency resolution implies a loss in time resolution that can be compensated by combining time aggregation with window overlapping, which is also useful for dealing with local peaks [21]. For example, the same time resolution is achieved with 0.4 s windows and a window

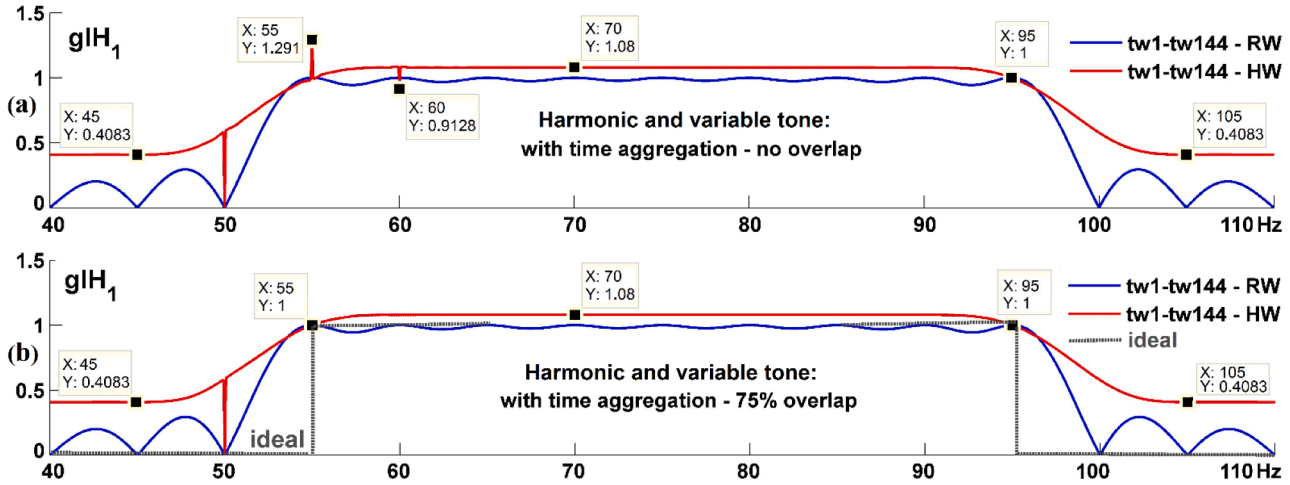

Fig. 9. Interharmonic group RMS values for a unit sweep tone and a fixed harmonic at 50 Hz, without aggregation with RW (blue) and aggregating over time with HW (red): (a) without overlap, and (b) with overlap of aggregated windows.

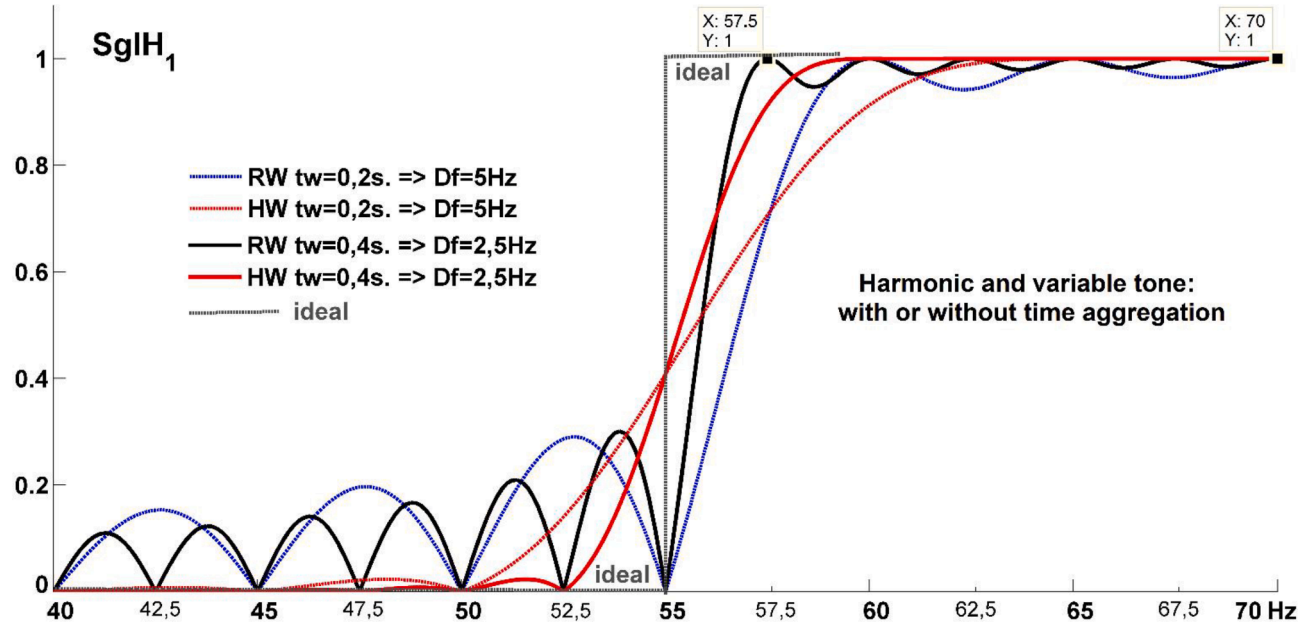

Fig. 10. Interharmonic subgroup RMS value for a sweep unit tone and a fixed harmonic at 50 Hz, for windows without aggregation and with different resolutions: RW at 5 Hz (dotted blue), RW at 2.5 Hz (black), HW at 5 Hz (dotted red) and HW at 2.5 Hz (red).

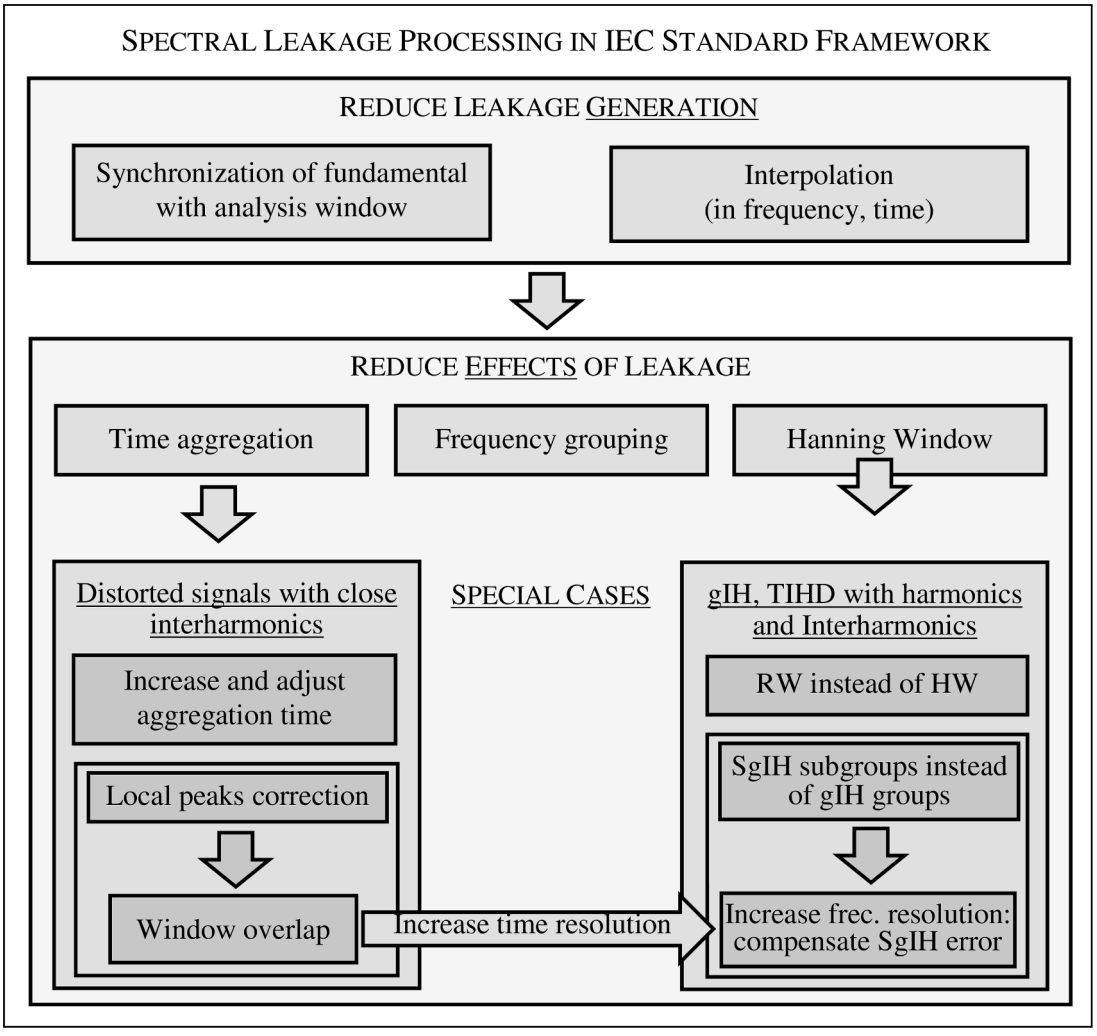

Fig. 11. Summary of the proposed methodology for processing spectral leakage in IEC standard framework.

overlap of 50%, than with 0.2 s windows without overlap. Another beneficial effect of increasing the sampling window time is the decrease of the synchronization error between the window and the fundamental harmonic and thus of the leakage due to this cause (at least, performing the synchronization with the zero-crossing detection method).

Fig. 11 summarizes the methodology described, starting with a reduction in the generation of the leakage from the moment the signal is sampled and the DFT is performed, and continuing with the procedures to reduce its effects once the leakage has been produced. Within these procedures, the two problematic situations raised in this article stand out: for signals with close interharmonics, the appropriate aggregation time must be increased and adjusted, in addition to using the overlap in time of the aggregated windows to correct in this way the local peaks that appear in the sensitivity curves; for the case of using HW in the measurement of interharmonic groups and rates, RW window can be better used in these cases, or subgroups and rates based on interharmonic subgroups can be used. In the latter case, the size of the sampling window can be extended, thus increasing the frequency resolution, to compensate for the loss of information that occurs when using subgroups instead of interharmonic groups.

4. Case study

This section presents and analyses the results obtained from various tests on an induction motor, with the aim of verifying the concepts developed above. A Siemens star-connected motor with rated values: 0.75 kW, 50 Hz, 400 V and 1.86 A was used, loaded with a magnetic powder brake, running both at low and high load (slip close to 0.3% and around 4%, respectively). To obtain a wider range of harmonic content, the induction motor was fed from two different converters, one with a sinusoidal PWM modulation (Allen Bradley PowerFlex 40) and the other with a random carrier frequency modulation (Telemecanique Altivar 66). The data were sampled at 80 kS/s using a National Instruments PCI6250 acquisition card and processed with Matlab software. The motor run in steady state for 60 s. Fig. 12 shows the laboratory test bench. The measurement point was the output of the converters, and it was therefore necessary to apply an analysis system adapted to the measurements at this point, using enhanced standardized measurement procedures.

Different groupings and distortion rates are used to demonstrate, with real measurements, the problems when making measurements based on the IEC standards, starting with the instability and inaccuracy of the values obtained when using inadequate aggregation times. In addition, the problem when measuring with HW will be verified, as well as its solution by performing measurements with subgroups and distortion rates based on interharmonic subgroups.

The groupings and distortion rates used in the results shown in this section are:

- gIH_1 and $sgIH_1$: 1st interharmonic group and subgroup, respectively. They measure the current or voltage RMS value, contained in the spectral bars between 1st and 2nd harmonic, not including the sidebars in the case of the subgroup.
- THD_{LF}: harmonic distortion rate considering the low part of the spectrum. It includes the sum of all squared harmonics, from the 2nd to the 40th inclusive, and is normalised by the fundamental frequency. This rate, like the previous groupings, is based on that defined in the standard [16], and all of them have been adapted to the possibility of working with fundamental frequencies different from those of the network, as occurs when a motor is supplied from an inverter.
- $TIHD_{LF}$ and $TIHDS_{LF}$: group and subgroup interharmonic distortion rates, respectively, considering the lower part of the spectrum. They include the sum of all interharmonic groups and subgroups squared up to and including the 40th and are normalised by the fundamental frequency. Since the standards do not define them, they have been based on rates proposed by some authors [47–49], adapting them to the measurement at the output of inverters.

In order to test the benefits of the measurement procedures, a situation with a high harmonic and interharmonic content across the whole spectrum was chosen. Measuring at the output of the converters ensures this in the high part of the spectrum. To achieve this at the low part, mixed eccentricity was induced in the tested motor (as shown in Fig. 13 for the PowerFlex inverter). Due to the eccentricity of the motor, a large interharmonic content is observed in this low-frequency part, and the related current groupings and rates (such as the interharmonic group gIH_1 in Fig. 13) are prone to be high. This higher interaction between tones requires to increase the aggregation time needed, as explained above. At high frequencies, the measurement of harmonics and interharmonics is not differentiated, because at high frequencies the synchronism of the acquisition window with the fundamental is usually lost

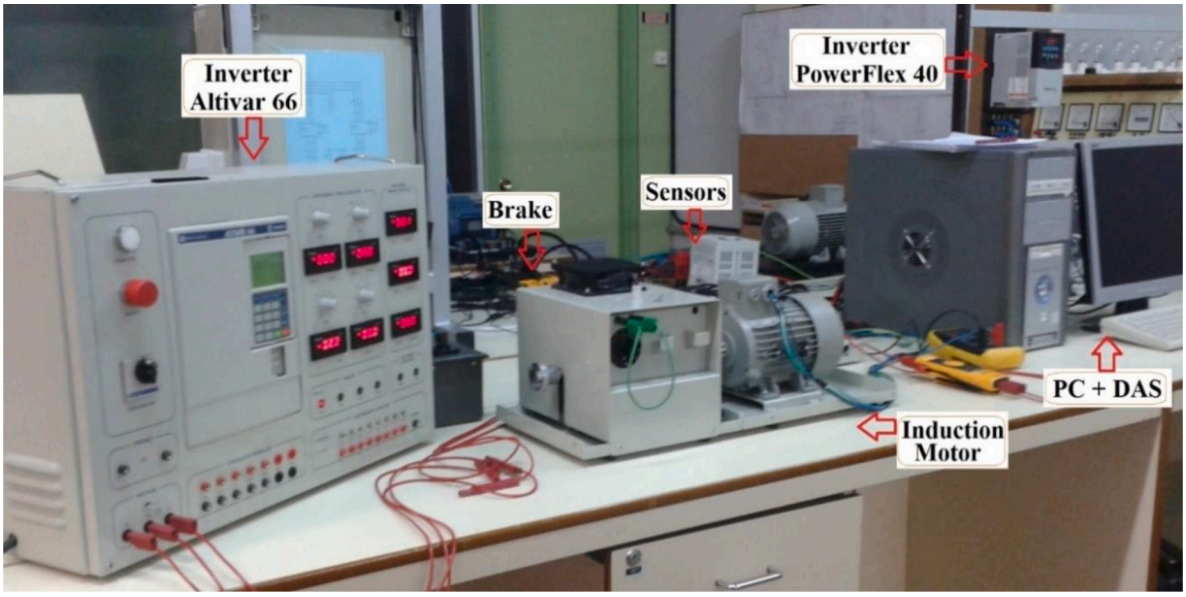

Fig. 12. Test rig used in the experiments.

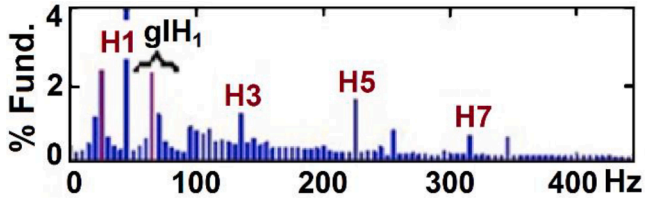

Fig. 13. Low frequencies range of the output current of the PowerFlex drive feeding an induction motor.

[47]. Therefore, the analysis made in this section is performed with practical cases with harmonics and interharmonics at low frequencies. Moreover, the relative magnitude of the harmonics is usually larger than that of the interharmonics at low frequencies (especially in the case of the fundamental harmonic), as shown in Fig. 13, making these cases more interesting for the problem raised by HW measurement with harmonics adjacent to the interharmonic groups.

The frequency response in Fig. 13 was obtained using the DFT, with spectral bars spaced 5 Hz apart. Similar tests were also carried out with the Altivar inverter and with the mains supply, obtaining spectra similar to the one shown in Fig. 13, so only the one obtained with the PowerFlex is shown as an example.

Fig. 14 presents the time evolution, using different types (RW - left plots, HW - right plots) and sizes of windows and degrees of overlap, of the RMS value of the interharmonic group gIH_1, measured at the output of the inverter of the same test as in Fig. 13. The lower plots (Fig. 14(b)) use windows of tw = 0.4 s (2.5 Hz resolution) and 0.2 s in the other plots. In the upper plots (Fig. 14(a)) no overlapping measurements are used and in the lower plots aggregation with 75% overlap is used. The graphs in red show the aggregated values up to each instant, so that the value of any aggregation size up to 60 s of the total test time can be observed.

From the values obtained in each individual window (blue plots in Fig. 14) the maximum and minimum values without aggregation are found and plotted in Fig. 15 (marked as "Max." and "min.", in red and blue, respectively). The aggregated values for time aggregations of 3 s and 10 s (in brown and turquoise, respectively) are also plotted. Fig. 15 also shows the results obtained with the Altivar drive and the mains supply.

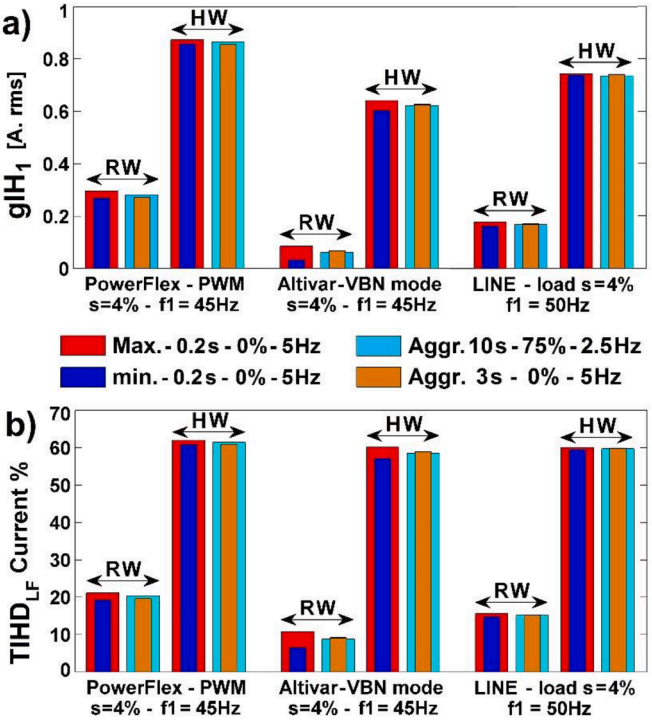

Fig. 15. Interharmonic group and interharmonic distortion group rate of the current of an induction motor fed from mains and from PowerFlex and Altivar drives, using different types and sizes of windows and degrees of overlap: (a) RMS value of gIH1 group, and (b) $TIHD_{LF}$ group rate for low frequencies.

Fig. 15 shows the different values obtained for interharmonic group gIH1 and for the distortion rate $TIHD_{LF}$ (which also contains interharmonic groups). In both cases there are adjacent harmonics that are not to be considered, and therefore presents an erroneous value using HW. Different resolutions or window sizes, aggregation times and degree of overlapping are used. In all cases, much higher values are

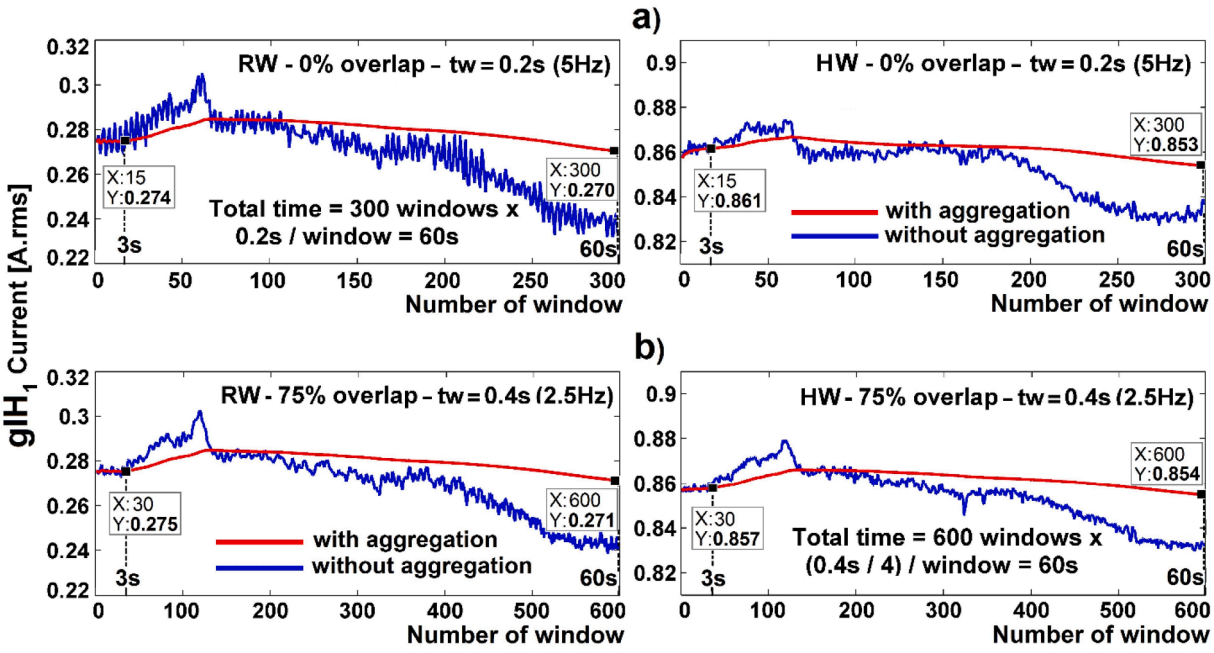

Fig. 14. Time evolution of the RMS value of the interharmonic group, gIH_1, of the PowerFlex drive, with RW (left graphs) and HW (right), in blue without aggregation, and in red with time aggregation: (a) without overlap and with 5 Hz resolution, and (b) with overlap and 2.5 Hz.

obtained with HW than with RW, due to the contribution of the sidebands of the harmonics adjacent to the interharmonic groups that make up the rate, this contribution being more relevant in the case of the fundamental harmonic.

5. Discussion

Analysing the results of the previous section, it can be observed that the results obtained with time aggregation are more stable than those without aggregation. Furthermore, with such signals (measured at the output of inverters driving faulted induction motors), with harmonics surrounded by a large interharmonic content (Fig. 13), it is observed that a longer aggregation time is necessary to stabilise the results. Thus, for example, observing the graphs in Fig. 14, it can be clearly seen that the 3 s aggregation time indicated by standard 61000–4–30 is insufficient to achieve a stable result, so it is advisable to increase this value at least for the analysed cases. Moreover, the maximum aggregation time is limited by the thermal constants of the equipment tested.

It is also observed that there are significant variations between the individual window values for interharmonic groupings. This is due to the leakage produced by the interharmonics which causes them to interact with each other, and thus requiring more aggregation time to stabilize these values.

Figs. 14 and 15 also show the problem described in Section 3.2 related to the higher value of the interharmonic group (and of the distortion rates containing interharmonic groups) found with HW compared to RW. It seems clear that such higher value is due to the presence of harmonics adjacent to the measured interharmonic groups. Therefore, one solution to the error due to harmonic sidebands when using HW may be to use RW. Another solution is to skip the spectral bars adjacent to the harmonics by better using subgroups instead of interharmonic groups, which can also increase the frequency resolution to compensate for the loss of information due to not including the bars adjacent to the harmonics. In Fig. 16 subgroups are used instead of interharmonic groups and it can be seen that the results obtained with HW are more similar to those found with RW, as expected, as opposed to the differences seen in Fig. 15 if interharmonic groups are used.

This problem when using HW does not occur however when measuring distortion rates that only include harmonics, such as THD_{LF}, since in those cases the unwanted sidebands are not considered, as they are located in the space between consecutive harmonics that are not taken into account for calculating THD. This is the case for the current distortion rate shown in Fig. 17 using different types and sizes of windows and degrees of overlap, for the same tests as in the previous figures. It can be seen that the differences between using RW and HW are not so significant and sometimes even the result obtained with HW is lower. The differences between using RW and HW are also reduced increasing the aggregation time, as can be seen by comparing the graphs for unaggregated values (Max. and min. in red and blue) with those aggregated for 3 and 10 s (in brown and turquoise). To find the THD rate, non-consecutive spectral bars are added, so in this case the group gain [19], value $\sqrt{1.5}$, is not used to correct the result in case of using HW.

Neither does HW present problems due to the inclusion of unwanted sidebands when measuring rates that include consecutive spectral bars, since in these cases it is of interest to measure all the bands of HW, including the sidebands. In these cases the group gain is used to correct the values obtained with HW. An example of this type of rate, which includes consecutive spectral bars, and therefore does not present problems when using HW, is the calculation of the total RMS value of the signal, found as the sum of all the spectral bars (Parseval's theorem). Here again, there is no major difference between using HW and RW, as shown in Fig. 18.

The increase in the analysis window and, therefore, the improvement of the frequency resolution, as well as the increase of the aggregation time to improve the stability and accuracy of the measurements, imply more processing time for analysing the data, but the hardware required would be similar to that used in commercial power quality meters IEC-based. On the contrary, if other more precise methods are used for interharmonics measurement, such as parametric methods, these require a higher computational cost and a previous knowledge of the harmonic content to be measured, which is lacking when measuring signals with unpredictable harmonic contents such as those present in the outputs of the power converters considered in this article.

6. Conclusions

Power quality measurement standards in the IEC framework establish procedures for minimizing the effects of spectral leakage on harmonic distortion measurement, describing both the frequency groupings and the necessary time aggregations. However, such procedures are not

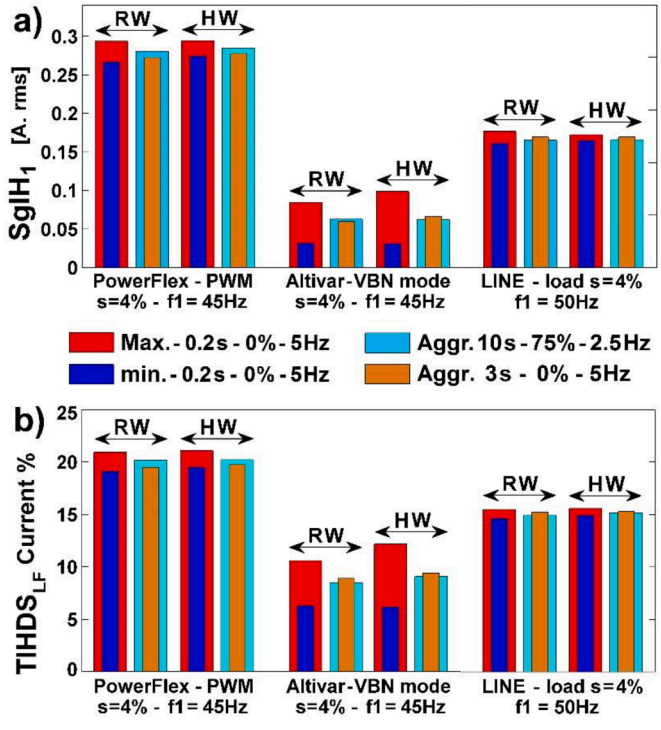

Fig. 16. Interharmonic subgroup and interharmonic distortion subgroup rate of the current for the same tests of Fig. 15, using different types and sizes of windows and degrees of overlap: (a) RMS value of SgIH1 subgroup, and (b) $TIHDS_{LF}$ subgroup rate for low frequencies.

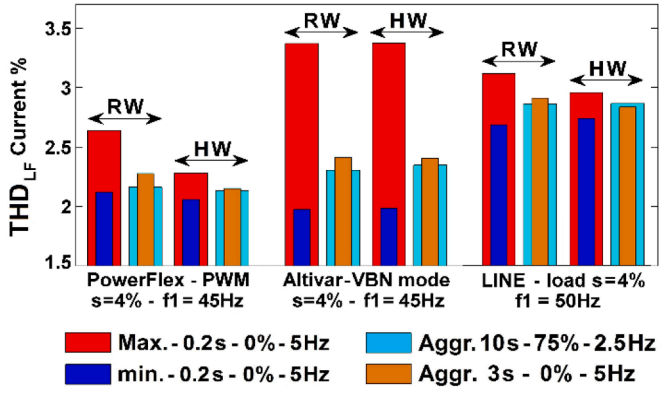

Fig. 17. Harmonic current distortion rate for low frequencies, THD_{LF}, for the same tests as in the previous figures, with different types and sizes of windows and degrees of overlap.

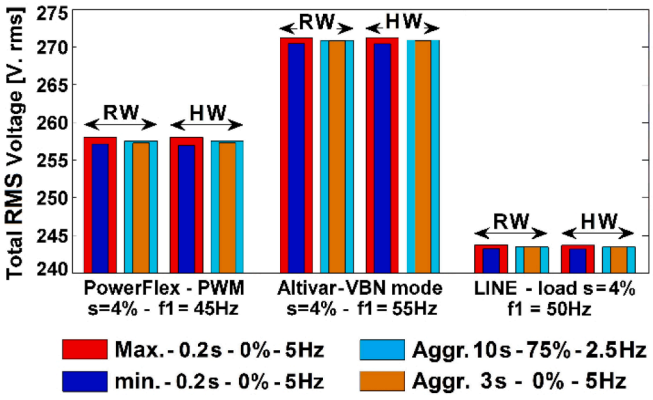

Fig. 18. Total RMS voltage value, for tests as in the previous figures, with different types and sizes of windows and degrees of overlap.

sufficiently accurate when, due either to the presence of interharmonics or to fundamental desynchronization, the length of the chosen time window is not an integer multiple of the periods of all the components contained in the signal, generating in these cases spectral leakage producing misleading measurements of the harmonic content. A common case in which this situation occurs is the operation of inverter-fed induction motors.

This paper demonstrates that, as a result of spectral leakage, two problems occur in the measurement of harmonic distortion based on the IEC standards. One problem is the variability and inaccuracy of the RMS values found in successive sampling windows after applying the DFT, when close tones interact, due to spectral leakage produced by at least one of them. These variations affect the IEC standards frequency groupings and distortion rates. In addition, for the case of using HW (according to the standard, usable for cases of loss of synchronism), a second problem appears: the interharmonic groups (and distortion rates containing them) can absorb part of the energy of their adjacent harmonics, due to the sidebands of HW, giving rise to erroneous measurements.

To solve these problems, this paper has presented a methodology to improve the accuracy of the harmonic distortion measurement process in the IEC Standard Framework, and the conclusions reached are as follows:

- The problem that arises when several close tones interact is solved by performing time aggregation to minimise the effects of the leakage on the resulting amplitude variation, and thus to obtain a more reliable and stable common RMS value. Such time aggregation must be applied to all groups and subgroups, harmonics and interharmonics, and to all distortion rates, since these rates are composed of such normalized frequency groupings.
- To solve the problem where interharmonic groups may absorb part of the energy of their adjacent harmonics as a consequence of using HW, it is concluded that it is preferable to use either the RW or distortion rates using interharmonic subgroups, thereby bypassing the sidebands to the harmonics that are not to be measured.
- In contrast, it has been found that the latter problem, associated with HW, does not occur when measuring frequency groupings and distortion rates containing all spectral bars, including harmonics, or when measuring only harmonics.
- An increase in frequency resolution can compensate for the loss of accuracy due to the use of interharmonic subgroups instead of groups, if HW is used. Increasing the frequency resolution also improves the overall resolution of the rest of the parameters, obtaining responses closer to the ideal, and also reduces the errors due to the synchronization between the fundamental and the sampling window and consequently reduces the generation of spectral leakage.
- The loss of time resolution (due to the increase in frequency resolution) can be partly corrected thanks to the use of window overlapping, which is also necessary to resolve the local peaks that appear in certain positions of the tones.

Finally, future research will need to continue investigating the window sizes that determine the most appropriate frequency and time resolutions, as well as the aggregation times that optimally minimise the effects of leakage, in order to improve the accuracy of harmonic distortion measurements. This selection of parameters should be a function of the harmonic and interharmonic content and degree of stationarity of the analysed signals, since the values used by current techniques based on standards use fixed resolutions and constant aggregation sizes, which can lead to problems of instability and inaccuracy in the measurements of signals with high interharmonic content, like those present in modern power electronics-based devices.

CRediT author statement

Angel Arranz-Gimon: Conceptualization, Methodology, Software, Writing, Data curation

Angel Zorita-Lamadrid: Supervision, Data curation, Validation, Writing

Daniel Morinigo-Sotelo: Conceptualization, Methodology, Supervision

Oscar Duque-Perez: Validation, Supervision, Writing- Reviewing and Editing

Declaration of Competing Interest

The authors declare that they have no known competing financial interests or personal relationships that could have appeared to influence the work reported in this paper.

References

[1] E. Hossain, M.R. Tur, S. Padmanaban, S. Ay, I. Khan, Analysis and mitigation of power quality issues in distributed generation systems using custom power devices, IEEE Access 6 (2018) 16816–16833, https://doi.org/10.1109/ACCESS.2018.2814981.

[2] S. Rönnberg, M. Bollen, Power quality issues in the electric power system of the future, Electr. J. 29 (2016) 49–61, https://doi.org/10.1016/j.tej.2016.11.006.

[3] V. Ravindran, T. Busatto, S.K. Ronnberg, J. Meyer, M.H.J. Bollen, Time-varying interharmonics in different types of grid-tied PV inverter systems, IEEE Trans. Power Deliv. 35 (2020) 483–496, https://doi.org/10.1109/TPWRD.2019.2906995.

[4] D.A. Elvira-Ortiz, D. Morinigo-Sotelo, O. Duque-Perez, R.A. Osornio-Rios, R. J. Romero-Troncoso, Study of the harmonic and interharmonic content in electrical signals from photovoltaic generation and their relationship with environmental factors, J. Renew. Sustain. Energy. 11 (2019) 43502, https://doi.org/10.1063/1.5094038.

[5] L.P. Moura, A. Reis, M.D.S. Lima, J.C. De Oliveira, I.N. Santos, Experimental evaluation of wind turbines inverters on generating harmonic currents, Int. J. Emerg. Electr. Power Syst. 20 (2019), https://doi.org/10.1515/ijeeps-2018-0210.

[6] A.J. Collin, S.Z. Djokic, J. Drapela, Z. Guo, R. Langella, A. Testa, N.R. Watson, Analysis of approaches for modeling the low frequency emission of LED lamps, Energies 13 (2020) 1571, https://doi.org/10.3390/en13071571.

[7] J. Garrido, A. Moreno-Munoz, A. Gil-de-Castro, V. Pallares-Lopez, T. Morales-Leal, Supraharmonics emission from LED lamps: a reduction proposal based on random pulse-width modulation, Electr. Power Syst. Res. 164 (2018) 11–19, https://doi.org/10.1016/j.epsr.2018.07.032.

[8] Â. Casaleiro, R.A.e Silva, B. Teixeira, J.M. Serra, Experimental assessment and model validation of power quality parameters for vehicle-to-grid systems, Electr. Power Syst. Res. 191 (2021), 106891, https://doi.org/10.1016/j.epsr.2020.106891.

[9] J. Baraniak, J. Starzyński, Modeling the impact of electric vehicle charging systems on electric power quality, Energies 13 (2020) 3951, https://doi.org/10.3390/en13153951.

[10] J. Meyer, V. Khokhlov, M. Klatt, J. Blum, C. Waniek, T. Wohlfahrt, J. Myrzik, Overview and classification of interferences in the frequency range 2-150kHz (Supraharmonics), in: SPEEDAM 2018 - Proc. Int. Symp. Power Electron. Electr. Drives, Autom. Motion, 2018, pp. 165–170, https://doi.org/10.1109/SPEEDAM.2018.8445344.

[11] D. Ritzmann, S. Lodetti, D. De La Veg, V. Khokhlov, A. Gallarreta, P. Wright, J. Meyer, I. Fernandez, D. Klingbeil, Comparison of measurement methods for 2-

150-kHz conducted emissions in power networks, IEEE Trans. Instrum. Meas. 70 (2021) 1–10, https://doi.org/10.1109/TIM.2020.3039302.
[12] A.A. Alkahtani, S.T.Y. Alfalahi, A.A. Athamneh, A.Q. Al-Shetwi, M. Bin Mansor, M. A. Hannan, V.G. Agelidis, Power quality in microgrids including supraharmonics: issues, standards, and mitigations, IEEE Access 8 (2020) 127104–127122, https://doi.org/10.1109/ACCESS.2020.3008042.
[13] M.J. Ghorbani, H. Mokhtari, Impact of harmonics on power quality and losses in power distribution systems, Int. J. Electr. Comput. Eng. 5 (2015) 166–174, https://doi.org/10.11591/ijece.v5i1.pp166-174.
[14] S. Khan, B. Singh, P. Makhija, A review on power quality problems and its improvement techniques, in: 2017 Innov. Power Adv. Comput. Technol. i-PACT, 2017, pp. 1–7, https://doi.org/10.1109/IPACT.2017.8244882, 2017-Janua (2018).
[15] A. Otcenasova, A. Bolf, J. Altus, M. Regula, The influence of power quality indices on active power losses in a local distribution grid, Energies 12 (2019) 1389, https://doi.org/10.3390/en12071389.
[16] International Electrotechnical Commission (IEC), IEC Standard 61000-4-7: General Guide On Harmonics and Interharmonics Measurements, For Power Supply Systems and Equipment Connected Thereto, IEC, Geneva, Switzerland, 2004. + A1:2010., (n.d.
[17] International Electrotechnical Commission (IEC), IEC Standard 61000-4-30: Testing and Measurement Techniques—Power Quality Measurement Methods, ed., IEC, Geneva, Switzerland, 2015.
[18] D. Gallo, R. Langella, A. Testa, On the processing of harmonics and interharmonics in electrical power systems, in: 2000 IEEE Power Eng. Soc. Conf. Proc 3, 2000, pp. 1581–1586, https://doi.org/10.1109/PESW.2000.847578.
[19] A. Testa, D. Gallo, R. Langella, On the processing of harmonics and interharmonics: using hanning window in standard framework, IEEE Trans. Power Deliv. 19 (2004) 28–34, https://doi.org/10.1109/TPWRD.2003.820437.
[20] T. Tarasiuk, A few remarks about assessment methods of electric power quality on ships – present state and further development, Measurement 42 (2009) 1153–1163, https://doi.org/10.1016/j.measurement.2008.02.003.
[21] A. Arranz-Gimon, A. Zorita-Lamadrid, D. Morinigo-Sotelo, O. Duque-Perez, A study of the effects of time aggregation and overlapping within the framework of IEC standards for the measurement of harmonics and interharmonics, Appl. Sci. 9 (2019) 4549, https://doi.org/10.3390/app9214549.
[22] M.H.J. Bollen, I.Y.H. Gu, Signal processing of power quality disturbances, 2005. https://doi.org/10.1002/0471931314.
[23] P.F. Ribeiro, Time-varying waveform distortions in power systems, 2009. https://doi.org/10.1002/9780470746752.
[24] J. Bartman, B. Kwiatkowski, The influence of measurement methodology on the accuracy of electrical waveform distortion analysis, Meas. Sci. Rev. 18 (2018) 72–78, https://doi.org/10.1515/msr-2018-0011.
[25] B. Peterson, A.M. Blanco, J. Rens, J. Meyer, G. Botha, J. Desmet, Impact of aggregation interval on harmonic phase angle measurements, in: 9th IEEE Int. Work. Appl. Meas. Power Syst. AMPS 2018 - Proc, 2018, pp. 1–6, https://doi.org/10.1109/AMPS.2018.8494857.
[26] G. Foskolos, K. Lundengard, The impact of aggregation interval on current harmonic simulation of aggregated electric vehicle loads, in: Proc. Int. Conf. Harmon. Qual. Power, ICHQP, 2020, https://doi.org/10.1109/ICHQP46026.2020.9177899, 2020-July.
[27] A. Bracale, G. Carpinelli, Z. Leonowicz, T. Lobos, J. Rezmer, Measurement of IEC groups and subgroups using advanced spectrum estimation methods, IEEE Trans. Instrum. Meas. 57 (2008) 672–681, https://doi.org/10.1109/TIM.2007.911701.
[28] T. Tarasiuk, Comparative study of various methods of DFT calculation in the wake of IEC standard 61000-4-7, IEEE Trans. Instrum. Meas. 58 (2009) 3666–3677, https://doi.org/10.1109/TIM.2009.2019308.
[29] H.L. Moreira Monteiro, L.R. Manso Silva, C.A. Duque, L.M. De Andrade Filho, P. Fernando Ribeiro, Comparison of interpolation methods in time and frequency domain for the estimation of harmonics and interharmonics according to IEC standard, in: Proc. Int. Conf. Harmon. Qual. Power, ICHQP, 2014, pp. 1–5, https://doi.org/10.1109/ICHQP.2014.6842892.
[30] V. Khokhlov, J. Meyer, A. Grevener, T. Busatto, S. Ronnberg, Comparison of measurement methods for the frequency range 2-150 kHz (Supraharmonics) based on the present standards framework, IEEE Access 8 (2020) 77618–77630, https://doi.org/10.1109/ACCESS.2020.2987996.
[31] T. Mendes, C. Duque, L. MansodaSilva, D. Ferreira, J. Meyer, P. Ribeiro, Comparative analysis of the measurement methods for the supraharmonic range, Int. J. Electr. Power Energy Syst. 118 (2020), https://doi.org/10.1016/j.ijepes.2019.105801.
[32] A.J. Collin, R. Langella, A. Testa, Assessing distortion within the IEC framework in the presence of high frequency components : some considerations on signal processing, in: 2018 IEEE 9th Int. Work. Appl. Meas. Power Syst, 2018, pp. 1–6, https://doi.org/10.1109/AMPS.2018.8494869.
[33] C.I. Chen, Y.C. Chen, Comparative study of harmonic and interharmonic estimation methods for stationary and time-varying signals, IEEE Trans. Ind. Electron. 61 (2014) 397–404, https://doi.org/10.1109/TIE.2013.2242419.
[34] A.M. Stanisavljević, V.A. Katić, B.P. Dumnić, B.P. Popadić, Overview of voltage dips detection analysis methods, in: 19th Int. Symp. Power Electron. Ee 2017. 2017-Decem, 2017, pp. 1–6, https://doi.org/10.1109/PEE.2017.8171703.
[35] S.K. Jain, S.N. Singh, Harmonics estimation in emerging power system: key issues and challenges, Electr. Power Syst. Res. 81 (2011) 1754–1766, https://doi.org/10.1016/j.epsr.2011.05.004.
[36] W.R. Oliveira, A.L.F. Filho, J. Cormane, A contribution for the measuring process of harmonics and interharmonics in electrical power systems with photovoltaic sources, Int. J. Electr. Power Energy Syst. 104 (2019) 481–488, https://doi.org/10.1016/j.ijepes.2018.07.018.
[37] Union of the Electricity Industry Eurelectric, Application Guide to the European Standard EN 50160 On "Voltage Characteristics of Electricity Supplied By Public Distribution Systems", ed., Electricity Product Characteristics and Electromagnetic Compatibility, Ref, 23002Ren9530, 1995.
[38] D. Gallo, R. Langella, A. Testa, Double stage harmonic and interharmonic processing technique, in: Proc. IEEE Power Eng. Soc. Transm. Distrib. Conf 2, 2000, pp. 1141–1146, https://doi.org/10.1109/pess.2000.867540.
[39] J. Barros, R.I. Diego, On the use of the Hanning window for harmonic analysis in the standard framework, IEEE Trans. Power Deliv. 21 (2006) 538–539, https://doi.org/10.1109/TPWRD.2005.852339.
[40] J. Barros, R.I. Diego, Effects of windowing on the measurement of harmonics and interharmonics in the IEC standard framework, in: Conf. Rec. - IEEE Instrum. Meas. Technol. Conf., 2006, pp. 2294–2299, https://doi.org/10.1109/IMTC.2006.235205.
[41] H. Soltani, P. Davari, F. Zare, F. Blaabjerg, Effects of modulation techniques on the input current interharmonics of adjustable speed drives, IEEE Trans. Ind. Electron. 65 (2018) 167–178, https://doi.org/10.1109/TIE.2017.2721884.
[42] K. Lee, G. Shen, W. Yao, Z. Lu, Performance characterization of random pulse width modulation algorithms in industrial and commercial adjustable-speed drives, IEEE Trans. Ind. Appl. 53 (2017) 1078–1087, https://doi.org/10.1109/TIA.2016.2616407.
[43] W. Zhang, Y. Xu, J. Ren, J. Su, J. Zou, Synchronous random switching frequency modulation technique based on the carrier phase shift to reduce the PWM noise, IET Power Electron 13 (2020) 892–897, https://doi.org/10.1049/iet-pel.2019.0642.
[44] Y.G. Gao, F.Y. Jiang, J.C. Song, L.J. Zheng, F.Y. Tian, P.L. Geng, A novel dual closed-loop control scheme based on repetitive control for grid-connected inverters with an LCL filter, ISA Trans 74 (2018) 194–208, https://doi.org/10.1016/j.isatra.2018.01.029.
[45] Y. Merizalde, L. Hernández-Callejo, O. Duque-Perez, State of the art and trends in the monitoring, detection and diagnosis of failures in electric induction motors, Energies 10 (2017) 1056, https://doi.org/10.3390/en10071056.
[46] P. Gangsar, R. Tiwari, Signal based condition monitoring techniques for fault detection and diagnosis of induction motors: a state-of-the-art review, Mech. Syst. Signal Process. 144 (2020), 106908, https://doi.org/10.1016/j.ymssp.2020.106908.
[47] A. Arranz-Gimon, A. Zorita-Lamadrid, D. Morinigo-Sotelo, O. Duque-Perez, A Review of Total Harmonic Distortion Factors For the Measurement of Harmonic and Interharmonic Pollution in Modern Power Systems, 14, Energies, 2021, p. 6467, https://doi.org/10.3390/EN14206467. Page14 (2021) 6467.
[48] H. Soltani, F. Blaabjerg, F. Zare, P.C. Loh, Effects of passive components on the input current interharmonics of adjustable-speed drives, IEEE J. Emerg. Sel. Top. Power Electron. 4 (2016) 152–161, https://doi.org/10.1109/JESTPE.2015.2505306.
[49] R. Langella, A. Testa, J. Meyer, F. Moller, R. Stiegler, S.Z. Djokic, Experimental-based evaluation of PV inverter harmonic and interharmonic distortion due to different operating conditions, IEEE Trans. Instrum. Meas. 65 (2016) 2221–2233, https://doi.org/10.1109/TIM.2016.2554378.